Taiwan Photon Source Towards User Operation

During the commissioning of a new light source, the measured beam parameters and functions of components are verified or tested according to the specifications of the lattice design and hardware. If tests show the results to be matched satisfactorily to the designed values, they are deemed acceptable and installation is completed without problem. This paragon seldom appears because foresight is incomplete. To diminish the difficulty and uncertainty caused from an extremely tight schedule of installation, the commissioning of the TPS was divided into phase I and phase II. In phase-I commissioning, the main goals were to measure the beam parameters and to accomplish vacuum cleaning to be ready for installation of two SRF cavities, and to gain sufficient experience for TPS commissioning in phase II. In that commissioning, ten insertion devices, two SRF cavities and seven beamlines had to be tested and verified to achieve their designed performance.

The TPS accelerator tunnel includes a storage ring and a booster ring; a transfer line connects the storage ring and the booster (BTS). Located in an independent room, a pre-injector comprises a 90-keV thermionic electron gun, 150-MeV Linac system and a Linac-to-booster transfer line (LTB). A safety metal shutter with interlock to the dipole current of the LTB prevents scattered electrons from entering the accelerator tunnel during the Linac commissioning period.

The 150-MeV electron beam is injected from the pre-injector through an injection septum to the booster ring; the injection kicker imposes a right-angle kick on the injected electron beam into the on-axis trajectory, and a five-cell RF cavity accelerates the electron beam with a synchronized magnetic field at repetition rate 3Hz. The two extraction kicker give the e-beam an angle kick through two extraction septum into BTS while the energy of electron beam reached 3 GeV. The BTS transfer line matches the beam parameters of the booster and the storage ring to ensure great efficiency of injection. The 3- GeV e-beam is injected through two injection septa to kickers 3 and 4 of the storage ring, incorporating the off-axis stored beam; the stored beam current accumulates.

During the beam commissioning, it is essential to obtain a stored beam and to minimize its closed-orbit distortion. Then linear optics are corrected and alignment of the beam corrects the engineering errors, which might have come from alignment error, accelerator components or a field error of the magnets. Beam parameters are compared between measured and designed values.

Table 1: Beam parameters of the Linac and booster.

Beam parameters of Linac	
Linac energy (MeV)	150
Beam emittance at 150 MeV ε_{nx} (πmm • mrad)	36
Energy spread at 150 MeV (% rms) multi-bunch	0.35
Beam parameters of booster	
Maximum energy (GeV)	3
Circumference (m)	496.8
Repetition rate (Hz)	3
Betatron tune ν_x/ν_y	14.38/9.302
Beam emittance εx (mm • mrad)	
RF frequency (MHz)	499.654
Synchrotron tune ν_s at 3 GeV	0.00861
Energy spread at 3 GeV (%)	0.095174
Horizontal/vertical beam clearance (mm)	17.5/10

To accommodate a beamline hutch, the enclosure of the liquid-nitrogen pipe, and installation of the beamline end stations, the radiation dose regulation was set to 2μSv/4 h. This setting ensures the radiation safety of all workers in the experimental hall during the beam commissioning in phases I and II.

Commissioning in phase I

The beam parameters of the 150-MeV Linac and the booster are shown in Table 1.

The booster beam commissioning began on August 12, 2014; it was delayed for three days because of a fire in the power supply of the booster dipole during AC-mode testing. The resistor of the leakage-current detector of the booster dipole PS was designed as 100 Ω with an insufficient safety margin, such that it became heated to more than 1000 °C and caused nearby circuits to burn during AC-mode testing. The resistance of the resistor was increased to 1 MΩ and extra cooling fans were added to take heat away from the cabinet of dipole power supply.

It took three months of struggle to bring the stored beam to 150 MeV, which was the first step of the booster beam commissioning. Several efforts were required, including improving the field uniformity of the injection kicker from 2 % to 0.4 %, re-aligning the booster vacuum chamber from ± 6 mm to less than ± 1 mm in the vertical plane, and improving the field uniformity with fixtures installed at both sides of the dipole magnets and the quadrupoles to ensure the accuracy of the gap between the chamber and the magnets. Roughly 30,000 cycles of the injected e-beam were achieved, as Fig. 1 shows; it seemed that the injected beam could not form a closed orbit, which means a stable motion of the electron beam. Figure 2 shows that the distribution of the radiation dose was measured in every dipole of the booster ring, which might be a possible explanation of the problem.

On using a strong magnet to touch the vacuum chamber of the booster ring on November 12, 2014, the vacuum chamber was found to be magnetic. It took one month to cut the vacuum chamber of the booster, for de-magnetization at 1050 °C and re-installation of the booster and pumping down.

The 150-MeV stored beam was obtained within two days; the injected beam survived 50 ms on December 11 and the stored beam was obtained after turning on the RF system the next day. To appreciate the stored beam in DC mode, the closed-orbit distortion was corrected from 1.3 mm rms to 0.84 mm rms in the horizontal plane, and from 0.047 mm rms to 0.031 mm rms in the vertical

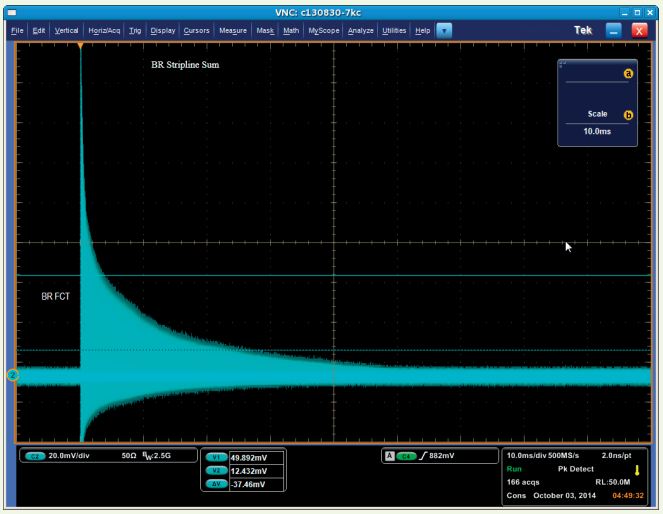

Fig. 1: The injected beam survived 35 ms with the RF on; the survival period was sensitive to the launching condition of the injected beam; the beam steering condition was irreproducible.

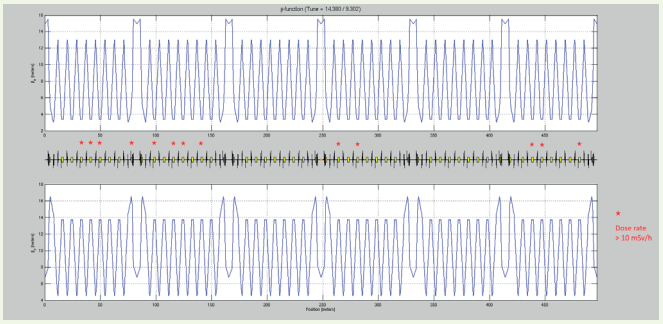

Fig. 2: Beta function of the booster in DC mode; a red star indicates the distribution of hot spots with a large radiation dose rate (> 10 mSv/h), implying that the linear optics were incorrect such that the injected electron beam could not attain a closed orbit.

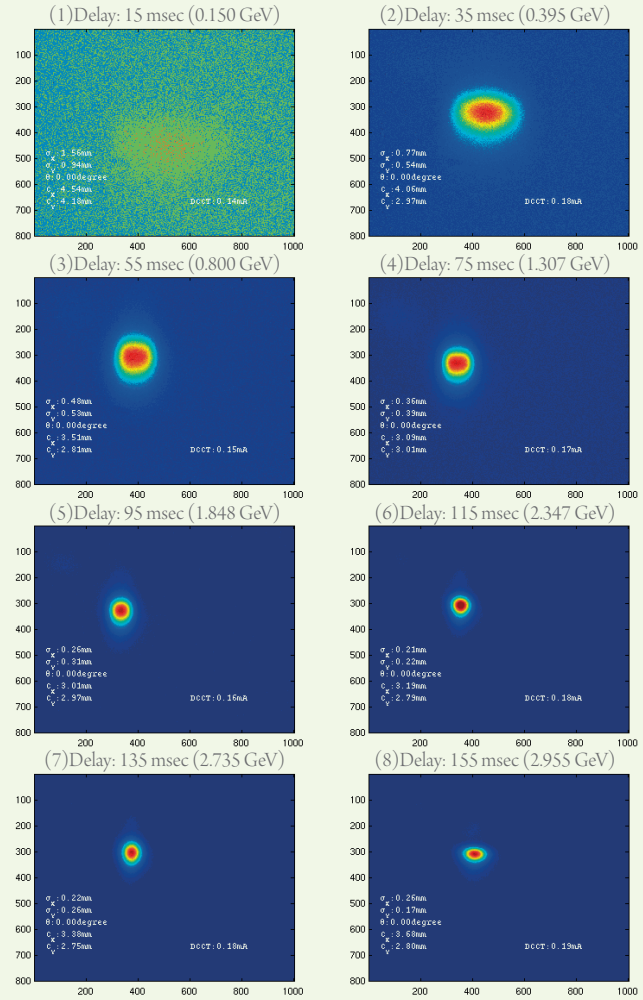

Fig. 3: It shows the synchrotron light profile from the booster electron beam during energy ramping; the 150-MeV beam profile is shown at top left and 3-GeV beam profile was showed at the bottom-right corner.

plane. The measured tuning and designed tuning were well matched; measured tuning $\nu_x = 14.381$ and $\nu_y = 9.268$, compared with designed tuning $\nu_x = 14.380$ and $\nu_y = 9.302$. After measuring beam parameters in the DC mode, commissioning of the energy ramping mode of the booster stored beam began on December 15, and the booster stored beam was successfully ramped up to 3 GeV on December 16. A proportional and time-shift compensation method was applied to the ramping waveform of the power supplies of the booster magnets, which included one dipole power supply, two families of sextuple power supplies, and four families of quadrupole power supplies. The working tuning compensation during energy ramping was also taken into account, and included in the waveform of the Q1 and Q2 power supplies. Figure 3 shows the variation of the beam size of the stored beam from 150 MeV ramped to 3 GeV.

The leakage field of the booster DC extraction septum became an obstacle in commissioning the storage ring; it affected the beam injected from Linac and the beam extracted from the booster. To test the functionality of the storage ring before installing the compensated correctors nearby the DC extraction septum, 1.5-GeV mode commissioning began on December 26; the stored beam was accumulated when beam parameters tuned to match the energy and storage ring circumference on December 29. After replacing several silicon-controlled rectifiers of the pulser of the injection septum, the commissioning of the storage ring at 3 GeV began on December 31; the stored beam accumulated to 5 mA only a few hours later. The machine parameters of the 3-GeV storage ring are presented in Table 2.

Table 2: Beam parameters of the storage ring.

Beam energy (GeV)	3
Circumference (m)	518.4
Beam current (mA)	500
Harmonic number	864
Beam emittance $\varepsilon_x/\varepsilon_y$ (nm • rad)	1.6/0.016
Betatron tuning ν_x/ν_y	24.18/13.28
Natural chromaticity (ξ_x/ξ_y)	-75/-26
Momentum compaction(α_1,α_2)	0.0024/0.0021
RF frequency (MHz)	499.654
RF voltage (MV)	2.8
Synchrotron tuning ν_s	5.42×10^{-3}
Radiation loss per tune (dipole only) (keV)	853.05

In commissioning in phase I, the maximum stored beam current attained 100 mA, which was nearly the safe maximum working power of the ceramic windows of the two five-cell PETRA cavities. The 35 A•Hour accumulated beam dose, an index of measurement of the vacuum cleaning, provided a satisfactory vacuum environment for installation of the two SRF cavities.

Table 3: Major parameters of ID for third-harmonic photons; only linear horizontal polarization mode is considered for EPU.

Port	ID	*E* (keV)	λ (mm)	Period	Gap (mm)	*By* (T)
05	IU22	5.7~20	22	140	5.6~10	1.02~0.48
09	IU22A	5.6~25	22	140	5.5~10	0.96~0.45
	IU22B	5.6~25	22	95	7~10	0.72~0.45
21	IUT22	7~25	22	140	5.5~10	0.98~0.46
23	IU22	4~15	22	140	5.5~10	0.95~0.45
25	IU22A	5~20	22	140	5.5~10	0.98~0.46
	IU22B	5~20	22	95	7~10	0.72~0.45
41	EPU48A*	0.22~1.5	48	68	13~40	0.84~0.14
	EPU48B*	0.22~1.5	48	68	13~40	0.84~0.14
45	EPU46*	0.28~1.5	46	82	14~37	0.79~0.16

* Horizontal linear mode.

Phase-II commissioning

Three major improvements of the accelerator components were made, including replacing the DC extraction septum with an AC extraction septum, decreasing the field strength of the injection septum and reinforcing the local shielding in the injection section, to diminish the obstacles on the way to phase II commissioning and toward user operation. The phase II beam commissioning began on September 14, 2015, on cleaning the vacuum chamber with photon-stimulated desorption with stored beam current 30 mA.

The re-measured beam parameters coincided with the beam parameters measured in March 2015. The ten insertion devices dedicated for seven beamlines were installed in seven straight sections. Table 3 shows details of the ID parameters and related positions.

To protect ID and the vacuum chamber from upstream synchrotron radiation because of a mis-steered electron beam, an orbit interlock was required. The orbit interlock criteria are shown in Table 4, which imply that the radiation slot in chamber B1 was too small. The radiation from EPU48 in the vertical polarization mode directly struck the radiation slot, depositing an enormous heat load on vacuum chamber B1 during high-current operation. Four B1 chambers required to be modified; it was decided to enlarge the radiation slot from 9 mm to 18 mm in October 2015.

A local problem of abnormal pressure occurred on October 4; the pressure in cell 2 increased exponentially once the stored beam current exceeded 180 mA. The vacuum leakage tests had been performed several times, including helium leak-testing with the stored beam; no leak was found, even on replacing the crotch absorber of chamber B1. An in-line replacement of cell 2 chamber B1 was performed in late November, which included in-line chamber cutting and welding. As a result, a tiny foreign matter was found inside the removed B1 chamber. This in-line replacement demonstrates satisfactory control of dust contamination, and the state-of-the-art vacuum cleaning approach without baking out. The stored beam current was raised to 520 mA on December 12, proving that the two RF systems and two SRF modules fully satisfied the power requirement for operation of the stored beam at current 500 mA. Figure 4 shows that the injection period was about 10 min to attain a stored beam current 520 mA.

Commissioning of the ID had to be postponed for two weeks because an unknown intense scattered light emitted on a YAG screen prevented aligning the upstream dipole with the ID by the synchrotron light, because the synchrotron light from the ID was hidden behind the unknown intense scattered light at the YAG screen. To prevent the aligned synchrotron light from bending and the ID from deflecting the electron beam orbit, the image provided alignment information about the ID before closing to its minimum gap to measure the feed-forward tables. YAK screen monitors are also placed in port 9 front end to visualize the relative location of bending magnet and ID..

To compensate the linear optical perturbations of insertion devices (ID), which included orbit feed-forward and tuning feed-forward for all ID, the coupling feed-forward was effected for EPU46, EPU48A and EPU48B only. The orbit distur-

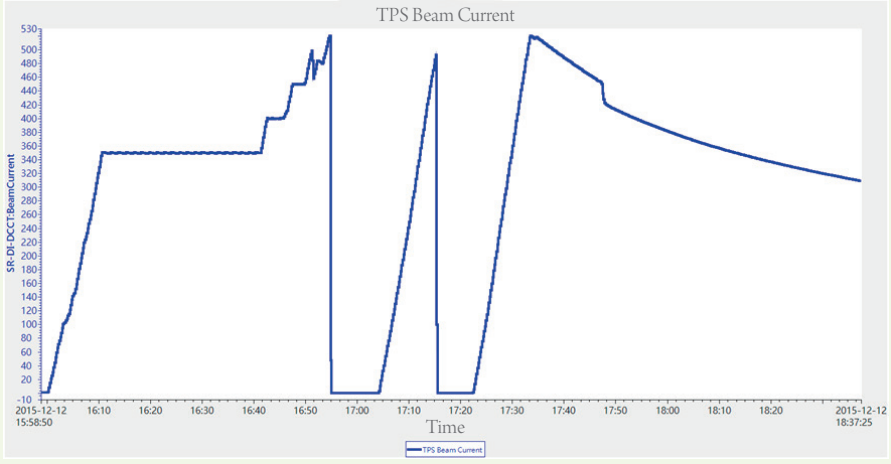

Fig. 4: It shows that it took about 10 min to accumulate stored beam current 520 mA.

Table 4: Criteria for the orbit interlock of various ID; a two-stage strategy was selected because of the large noise of BPM during injection. The orbit interlock windows of the upstream dipole of the IVU were set to ± 1 mm and ± 0.1 mm for horizontal and vertical planes respectively.

Port	Horizontal (mm)	Vertical (mm) first stage	Vertical (mm, mrad) second stage
5, 21, 23	± 1	± 0.1	(± 5, ± 0.4)
$09^{(B)}$, $25^{(B)}$	± 1	± 0.1	(± 5.5, ± 0.5)
$09^{(A)}$, $25^{(A)}$	± 1	± 0.1	(± 4.4, ± 0.24)
$46, 41^{(B)}$	± 1	± 0.1	(± 3.7, ± 0.34)
$41^{(A)}$	± 1	± 0.1	(± 1.15, ± 0.06)

(A) Upstream ID.
(B) Downstream ID.

Table 5: Comparison of orbit disturbance of ID without and with a feed-forward table. The reason for the poor performance of the feed-forward table for IU22A-09 is under investigation and requires further improvement.

Port	ID	Reference Gap (mm)	Minimum Gap (mm)	Max COD X/Y rms (um) before correction	Max COD X/Y rms (um) before correction	Max current of corrector [A]
05	IU22	40	5.6	39/6	0.5/0.1	0.33
21	IUT22	40	5.5	10/4	0.4/0.3	0.2
23	IU22	40	5.5	41/15	0.4/0.2	0.43
09	IU22A	40	5.5	75/6	0.5/1.5	0.6
	IU22B	40	7	16/5	0.3/0.2	0.15
25	IU22A	40	5.5	41/7	0.5/0.4	0.27
	IU22B	40	7	18/5	0.3/0.2	0.13
41	EPU48A	45	13	70/24	6.0/1.5	0.7
	EPU48B	45	13	137/29	4.5/1.3	1.6
45	EPU46	45	14	65/72	3.0/1.0	1.5

bance of each ID was minimized with two pairs of corrector magnets for horizontal and vertical correction at both its ends. The feed-forward table of the two pairs of correctors for the in-vacuum undulator depends on only the gap. The feed-forward table for the elliptical-polarization undulator depends on both the gap and the phase, so warranting a 2D table.

The tuning shift introduced by each ID is minimized with the two local nearby quadrupole pairs for tuning correction; the tuning feed-forward table is 1D for an in-vacuum undulator, but 2D for an EPU. The tuning feedback with two families of quadrupoles globally will be implemented to lock the working tuning. The skew error introduced by each EPU is minimized with long coil loops hung on the outside of the four-magnet array for the coupling correction; the feed-forward table is 2D.

A typical comparison of orbit disturbance of ID without and with feed-forward is presented in Table 5; the 2D coupling feed-forward table is shown in Fig. 5; the tuning shift of EPU48A is shown in Fig. 6.

Towards user operation

To achieve top-up operation with sub-micrometer stability of the electron orbit, the requirement of radiation safety must be fulfilled first, then, with completion of the system for machine protection, capabilities of the accelerator system and related reliability, and integrated performance of the accelerator complex.

The dose limit of the radiation monitor of TPS is 2 μSv/4 h, according to the principle of a reasonably achievable minimum, since the beginning of beam commissioning in phase I. The estimated radiation is 50 % γ-ray and 50 % neutrons, due to a 3-GeV injected electron beam loss; a reinforced local shielding wall was installed in the injection section during the shutdown period April to September, to provide the capability of operation at a large current during beam commissioning in phase II.

Optimization of the integrated performance of the accelerator complex will pave the way to successful user operation. The electron orbit interlock has been merged into a system for machine protection to protect ID and the vacuum chamber from radiation damage of a mis-steered electron beam,

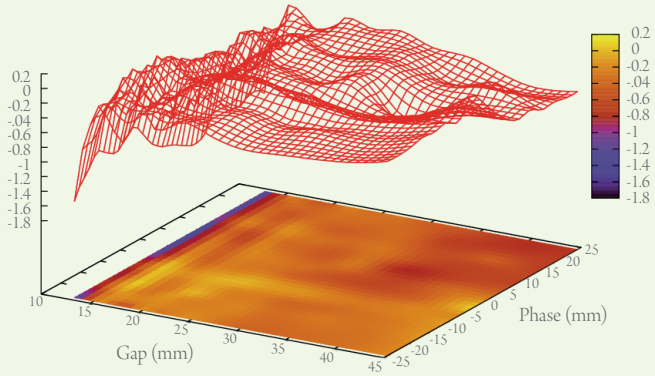

Fig. 5: Applied current of long coils shown on z-axis to compensate the skew quadrupole effect of EPU48A.

but at the cost of decreased accelerator availability. Any failure of BPM will, however, cause a false action of the orbit feedback, or a faulty BPM around an ID will activate the orbit interlock to cause a beam dump. It is crucial to mitigate false signals from critical components such as SRF modules, in-vacuum undulators and BPM, by delaying the response interval or decreasing the EMI noise. The reliability of accelerator components has been tested and improved during the period of beam commissioning, but the high performance of TPS user operation has still a long way to go; for instance, the beam trip diagnostics and failure analysis are not ready for user operation. (Reported by Yi-Chih Liu)

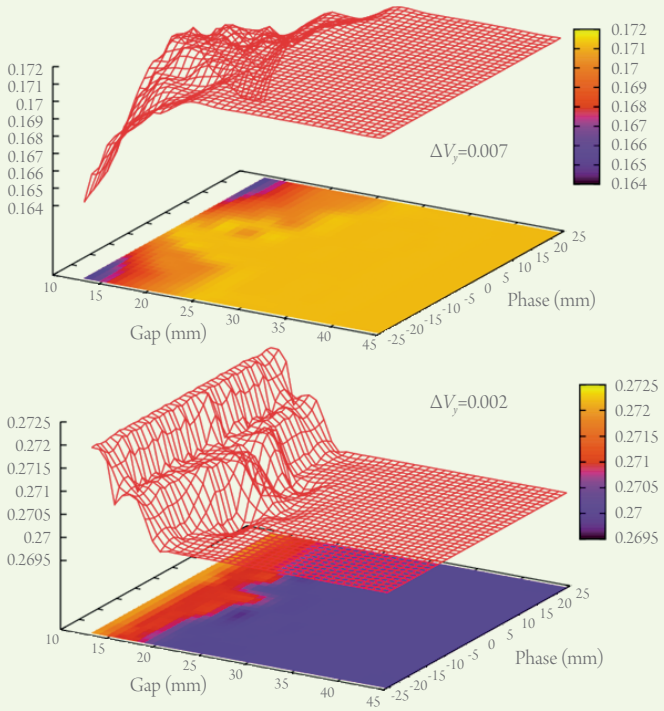

Fig. 6: (a) Horizontal fractal tuning was shown on the z-axis; the maximum horizontal tuning shift is 0.007. (b) Vertical fractal tuning was shown on the z-axis; the maximum vertical tuning shift is 0.002.

NEG Coating on Various UHV Chamber Materials

Surface outgassing is the main issue to achieve an ultrahigh-vacuum (UHV) status in an all-metal vacuum chamber. Much effort has been devoted to decrease surface outgassing, both using an appropriate surface treatment and elaborating on high-performance materials. Although physisorbed water can be removed by baking *ex situ*, residual gas still exists in a vacuum system; this gas consists of H_2, CO, CO_2 and CH_4 that result from bombardment of a surface by electrons, ions, energetic neutrals and synchrotron radiation.

When a gaseous molecule strikes a solid surface, multiple actions occur, including adsorption, desorption, surface reaction, back-scattering, diffusion and replacement, as shown in Fig. 1.[1] When adsorption of a gas occurs, the pressure decreases. The most important properties of materials that adsorb gases are chemical affinity and bulk diffusivity. Chemical affinity means that a residual gas becomes removed by chemical adsorption. Bulk diffusivity signifies that an adsorbed gas diffuses into the bulk of the materials. For the purpose of gas adsorption, many and diverse alloy systems have been studied in the hope of improving the performance of gas adsorption.

Coating with a thin film is proposed to be an improved method to decrease thermal outgassing and that induced by bombardment. Many coating materials have been tested for an application of ultra-high-vacuum technology. Among these various materials, a non-evaporable getter (NEG) as a thin film is best suited for pumping in a vacuum chamber with limited conductance.

The pumping mechanism of a NEG film involves surface adsorption followed by bulk diffusion. As the pumping speed of a NEG film for active gases is determined by its rate of diffusion into the bulk, we found that a NEG film requires activation, illustrated in Fig. 2.[2] Because inert gases or methane are not adsorbed on the NEG surface, they cannot be so pumped.

To achieve an ultra-high-vacuum (UHV) status, NEG films are hence introduced to absorb the components of the residual gas. NEG films have been developed at CERN for use in vacuum chambers of particle accelerators since 1995.[3,4]

NEG thin films have recently been coated onto the inner walls of vacuum chambers, or NEG strips have been mounted inside a vacuum chamber of a particle accelerator. For instance, the beam pipes of the ring of MAX IV, in Sweden, are coated with a Ti-Zr-V NEG thin film to fulfill the requirement of average pressure 1×10^{-7} Pa. NEG films have been deposited at CERN to coat pipes of various geometries. In the next paragraph, we discuss how getter materials are selected for application in pumping a vacuum system.

A selected getter material is characterized by possessing effective adhesion to the substrate, a large

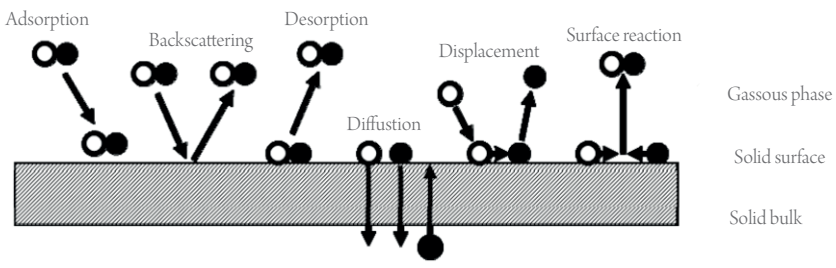

Fig. 1: Types of interaction between gas and surface.[1]